

# The Prosegment Catalyzes Pepsin Folding to a Kinetically Trapped Native State<sup>†</sup>

Derek R. Dee<sup>†</sup> and Rickey Y. Yada<sup>\*,‡,§</sup>

<sup>†</sup>*Biophysics Interdepartmental Group and* <sup>§</sup>*Department of Food Science, University of Guelph, Guelph, Ontario, Canada N1G 2W1*

*Received August 12, 2009; Revised Manuscript Received December 8, 2009*

**ABSTRACT:** Investigations of irreversible protein unfolding often assume that alterations to the unfolded state, rather than the nature of the native state itself, are the cause of the irreversibility. However, the present study describes a less common explanation for the irreversible denaturation of pepsin, a zymogen-derived aspartic peptidase. The presence of a large folding barrier combined with the thermodynamically metastable nature of the native state, the formation of which depends on a separate prosegment (PS) domain, is the source of the irreversibility. Pepsin is unable to refold to the native state upon return from denaturing conditions due to a large folding barrier (24.6 kcal/mol) and instead forms a thermodynamically stable, yet inactive, refolded state. The native state is kinetically stabilized by an unfolding activation energy of 24.5 kcal/mol, comparable to the folding barrier, indicating that native pepsin exists as a thermodynamically metastable state. However, in the presence of the PS, the native state becomes thermodynamically stable, and the PS catalyzes pepsin folding by stabilizing the folding transition state by 14.7 kcal/mol. Once folded, the PS is removed, and the native conformation exists as a kinetically trapped state. Thus, while PS-guided folding is thermodynamically driven, without the PS the pepsin energy landscape is dominated by kinetic barriers rather than by free energy differences between native and denatured states. As pepsin is the archetype of a broad class of aspartic peptidases of similar structure and function, and many require their PS for correct folding, these results suggest that the occurrence of native states optimized for kinetic rather than thermodynamic stability may be a common feature of protein design.

It is not unusual to observe that a protein is irreversibly unfolded; for example, this is often reported to be the case in DSC studies (1–3). However, the basis for such irreversibility may not be trivial (i.e., due to irreversible modification of the unfolded state) but may reveal fundamental elements of protein folding and stabilization mechanisms. Such is the case for  $\alpha$ -lytic peptidase ( $\alpha$ LP),<sup>1</sup> in which the native state was found to be less thermodynamically stable than the denatured and unfolded states (4). Another such example is pepsin. As a zymogen-derived protein, pepsin is initially produced at neutral pH as an inactive precursor form, termed pepsinogen, which contains an N-terminal, 44 amino acid prosegment (PS) domain. With increasing acidity, below pH 5, the PS is removed by hydrolysis (5) to result in mature, active pepsin ( $M_w$  34.6). Native pepsin (Np) is stable under acidic pH and has a bilobal conformation with two catalytic aspartic residues on either side of the active site cleft, formed between the N- and C-terminal domains (Figure 1). In pepsinogen, the PS is located inside this active site cleft. Curiously, while pepsinogen can be reversibly unfolded, pepsin is irreversibly denatured at neutral pH and does not refold to the native, active form upon acidification. For this reason native pepsin is known to be irreversibly denatured, a process that has been the subject of numerous studies (6–12).

Recent studies have revealed unusual aspects of pepsin denaturation by comparing the structures and stabilities of native,

alkaline denatured, and acid refolded porcine pepsin (Rp) (13). The stabilities and low-resolution secondary and tertiary structures of these states were characterized using differential scanning calorimetry, small-angle neutron scattering, and circular dichroism. Rp was shown to have secondary and tertiary structures intermediate between the alkaline denatured and native forms but was found to be thermodynamically more stable relative to Np, as evidenced by a reversible unfolding transition with a higher melting midpoint ( $T_m$ ). These data, therefore, strongly suggested that the irreversibility of pepsin denaturation was due to the native state existing as a thermodynamically metastable form.

The above finding brings to question how native pepsin is originally folded and stabilized. While it has been qualitatively understood that the PS is important for correct folding of aspartic peptidases, only for the serine peptidases  $\alpha$ LP and *Streptomyces griseus* peptidase B (SGPB) (4, 14–17) and subtilisin's E and BPN' (18–20), have there been quantitative studies to understand the requirement for and mechanism of the PS in folding. In the case of  $\alpha$ LP and SGPB, the PS has been shown to actively catalyze folding from the denatured state to the native state by lowering the free energy barrier to folding, enhancing the folding rate by as much as  $3 \times 10^9$  for  $\alpha$ LP and 400 times for SGPB (17). Once the PS is removed, the resulting native states are kinetically trapped, characterized by very slow unfolding and refolding rates, indicating a large energy barrier to unfolding/refolding in the absence of the PS. The PS was shown to act as a foldase for each of these enzymes; i.e., rather than preventing off-pathway folding events, as in the case of a chaperone, the PS directly catalyzes folding to the native state. Based on the finding that Rp was more stable than Np (13), it was hypothesized that the PS of pepsin functions in a similar manner. To examine this hypothesis, the folding/unfolding kinetics of pepsin were

<sup>†</sup>The financial support of the Natural Sciences and Engineering Research Council of Canada and the Canada Research Chairs Program is gratefully acknowledged.

<sup>\*</sup>Corresponding author. Tel: 519-824-4120 ext 58915. Fax: 519-824-6631. E-mail: ryada@uoguelph.ca.

<sup>1</sup>Abbreviations: PS, prosegment; PS<sub>p</sub>, synthetic prosegment peptide; Np, native pepsin; Rp, refolded pepsin;  $\alpha$ LP,  $\alpha$ -lytic peptidase; SGPB, *Streptomyces griseus* peptidase B; GdnHCl, guanidine hydrochloride.

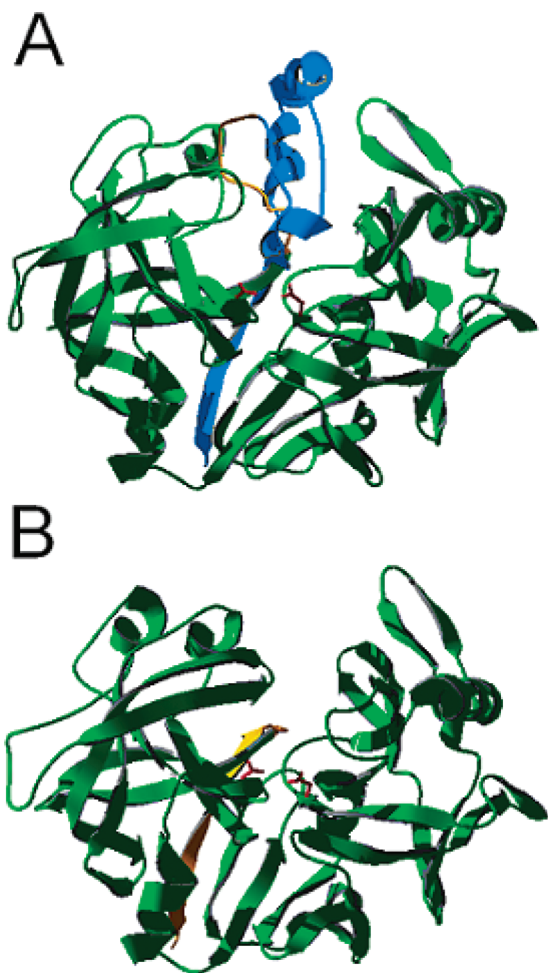


FIGURE 1: Crystal structures of (A) pepsinogen (PDB: 2PSG) and (B) pepsin (PDB: 3PEP). The prosegment (PS, blue) forms part of a six-stranded  $\beta$ -sheet plate and occludes the active site cleft in pepsinogen. After removal of the PS, residues 1–12 (orange) undergo a conformational change, with the mature N-terminus moving over 40 Å to form a strand within the six-stranded  $\beta$ -sheet plate, thus replacing the strand once formed by the PS. The catalytic Asp32 and Asp215 residues are shown in red.

measured and compared with the folding and interaction of pepsin when combined with a synthetic PS peptide ( $\text{PS}_p$ ). It was observed that the PS catalyzes the folding of pepsin and, once the PS is removed, a kinetically trapped native state is obtained. This finding explains the basis for pepsin irreversible denaturation and provides insight into how the PS facilitates correct folding of native pepsin.

## EXPERIMENTAL PROCEDURES

**Materials.** High-purity porcine pepsin A (EC 3.4.23.1) was purchased from Sigma (St. Louis, MO) and used without further purification. The peptide substrates KPAEFF( $\text{NO}_2$ )AL and MO-CAC-APAKFFRLK(Dnp)-NH<sub>2</sub> were purchased from Sigma Genosys (Oakville, Ontario, Canada) and from Peptide Institute, Inc. (Osaka, Japan), respectively. The synthetic 44-residue  $\text{PS}_p$  with C-terminal amidation (LVKVPLVRKKSRLRQNLKNG-KLKDFLKTHKHNPASKYFPEAAAL) was purchased from CanPeptide Inc. (Pointe-Claire, Quebec, Canada) and was more than 95% pure as judged by LC-MS. Protein stocks were prepared by mass (w/v), with concentrations determined by absorbance at 280 nm, using extinction coefficients of  $52830 \text{ M}^{-1} \text{ cm}^{-1}$

for pepsin and  $1490 \text{ M}^{-1} \text{ cm}^{-1}$  for prosegment, both of which were estimated using the ProtParam tool (21). Pepsin binding, folding, and unfolding experiments were carried out at pH 5.3 (20 mM acetic acid/NaOH buffer), as pepsin has been shown to display reduced proteolysis above pH 5 (22, 23).

**Refolded Pepsin Sample Preparation.** Alkaline denatured pepsin was prepared by making a 20 mg/mL solution in 30 mM NaOH, with a final pH of 8, and allowed to equilibrate for at least 10 min. Refolded pepsin (Rp) was then prepared by diluting an aliquot of the alkaline denatured protein to 0.35 mg/mL in 20 mM acetic acid/NaOH buffer with a final pH of 5.3.

**Uncatalyzed Pepsin Folding.** Rp samples were prepared (0.35 mg/mL) and incubated on ice (0 °C) in 20 mM acetic acid/NaOH buffer, pH 5.3, containing 100 mM NaCl. Aliquots were withdrawn at intervals from 0 to 4 days and assayed for hydrolytic activity using a sensitive fluorescence-based assay (detection limit <0.1 nM). The MOCAc-APAKFFRLK-(Dnp)-NH<sub>2</sub> substrate was used (excitation at 328 nm, emission at 393 nm), in which the quenching Dnp group is removed upon hydrolysis giving rise to an increase in fluorescence from MOCAc (24). Enzyme kinetics were measured at 25 °C in 20 mM phosphoric acid/NaOH buffer, pH 3.0, using a Shimadzu RF5301 spectrofluorophotometer (Shimadzu Corp., Kyoto, Japan). Initial reaction rates were determined from linear fits, corrected for background fluorescence, and used to calculate the amount of native pepsin recovered using a standard curve. Initial reaction rates were measured in triplicate at each time point, and the folding experiment was repeated four times.

**Inhibition Studies.** Pepsin hydrolysis of the KPAEFF-( $\text{NO}_2$ )AL substrate (25) was measured by following the decrease in absorbance at 300 nm using a Biochrom Ultrospec 3100-pro UV-vis spectrophotometer (Biochrom Ltd., Cambridge, England) at 25 °C in 20 mM acetic acid/NaOH buffer, pH 5.3, containing 100 mM NaCl. Np samples were diluted to 10 nM and incubated with  $\text{PS}_p$ , ranging in concentration from 0 to 480 nM, for 5 min at 25 °C and assayed for activity. The reaction rates were normalized to the activity in the absence of  $\text{PS}_p$  and the data fit using the competitive inhibitor form of the Michaelis–Menten equation

$$v_0 = \frac{V_{\max}[\text{S}]}{[\text{S}] + K_{\text{M}}(1 + [\text{I}]/K_{\text{i}})} \quad (1)$$

where  $v_0$  is the initial reaction rate,  $V_{\max}$  is the maximum reaction rate,  $[\text{S}]$  is the substrate concentration (fixed at 0.1 mM),  $[\text{I}]$  is the inhibitor concentration,  $K_{\text{M}}$  is the Michaelis constant, and  $K_{\text{i}}$  is the inhibition constant. Reaction rates were measured at least in triplicate for each  $\text{PS}_p$  concentration.

**Prosegment-Catalyzed Pepsin Folding.** Freshly prepared Rp solutions were diluted to  $\leq 1 \mu\text{M}$  in 20 mM acetic acid/NaOH buffer, pH 5.3, and 100 mM NaCl, and various amounts of  $\text{PS}_p$  were added, ranging from 3 to 40  $\mu\text{M}$   $\text{PS}_p$ , such that the ratio of  $\text{PS}_p$ :Rp was maintained at  $\geq 10:1$ . The solutions were incubated on ice (0 °C), and upon addition of  $\text{PS}_p$  to initiate the reaction, aliquots were taken at several time intervals, diluted in 50 mM phosphoric acid buffer, pH 1.1, incubated for 5 min at 25 °C, and assayed for Np activity using the UV substrate, KPAEFF-( $\text{NO}_2$ )AL. The recovery of Np activity at a single  $\text{PS}_p$  concentration was fit with a monoexponential function ( $y = a - b \exp(-k_{\text{f}}t)$ ) to obtain the folding rate,  $k_{\text{f}}$ . The  $k_{\text{f}}$  data were analyzed as a function of  $\text{PS}_p$  concentration according to the

modified Michaelis–Menten model, as used previously (15, 26) and described (19)

$$k_f = \frac{k_{\text{cat}}[\text{PS}_p]}{K_M + [\text{PS}_p]} \quad (2)$$

where  $k_{\text{cat}}$  is the maximum folding rate and  $[\text{PS}_p]$  is the concentration of  $\text{PS}_p$ .  $\text{PS}_p$ -catalyzed folding progress curves were determined at least in triplicate for each  $\text{PS}_p$  concentration.

**Prosegment Binding to Denatured Pepsin.** The change in the intrinsic tryptophan fluorescence of denatured pepsin upon binding  $\text{PS}_p$  was used to measure the affinity of the  $\text{PS}_p$  for Rp, a method that has been used to measure ligand binding for other proteins (27). Freshly prepared Rp solutions were diluted to 1.5  $\mu\text{M}$  in 20 mM acetic acid/NaOH buffer, pH 5.3, containing 100 mM NaCl, and mixed with various amounts of  $\text{PS}_p$ , ranging from 0 to 11  $\mu\text{M}$   $\text{PS}_p$ . After incubating the samples at 25 °C for  $\geq 20$  min, the intrinsic tryptophan fluorescence was measured using a Shimadzu RF5301 spectrofluorophotometer (Shimadzu Corp., Kyoto, Japan), with excitation at 295 nm and emission measured at 324 nm. The change in fluorescence,  $\Delta F_i$ , at each  $\text{PS}_p$  concentration was normalized relative to the maximum change,  $\Delta F_{\text{max}}$ , and fit according to

$$\Delta F_i / \Delta F_{\text{max}} = [\text{Rp}][\text{PS}_p] / (K_d + [\text{PS}_p]) \quad (3)$$

where  $[\text{Rp}]$  and  $[\text{PS}_p]$  are the concentrations of pepsin and  $\text{PS}_p$ , respectively, and  $K_d$  is the dissociation constant.  $\text{PS}_p$ -binding measurements were repeated five times.

**Kinetic Stability of Native Pepsin.** Unfolding was induced at a series of concentrations of guanidine hydrochloride (GdnHCl) in 20 mM acetic acid/NaOH at either 0 or 25 °C, using 1.5  $\mu\text{M}$  pepsin, and measured as the decrease in intrinsic tryptophan fluorescence (excitation at 295 nm, emission at 330 nm). Temperatures were maintained using a circulating water bath with either water or 20% MeOH/H<sub>2</sub>O (% w/w). The unfolding rate was obtained from a monoexponential fit of the data ( $y = a - b \exp(-k_u t)$ ), and a plot of the natural logarithm of the unfolding rate versus GdnHCl concentration was extrapolated to estimate the unfolding rate in the absence of denaturant. GdnHCl concentrations were measured by refractometry (28).

**Data Analysis.** All data analysis, including linear and non-linear curve fitting, was carried out using Origin v7.0 (OriginLab Corp., Northampton, MA).

## RESULTS

To quantify the effect of the PS on the pepsin folding landscape, it was necessary to assess the kinetic and thermodynamic stability of native pepsin. In addition to measuring the contribution of the  $\text{PS}_p$  to pepsin folding, the interactions of the  $\text{PS}_p$  with Rp and Np were also examined. Together, these data support and outline the function of the PS as a foldase, allowing for the formation of the Np state.

While screening for optimal conditions to follow  $\text{PS}_p$ -catalyzed folding of pepsin, measurements were made with and without 100 mM NaCl added to the buffer. As the recovery of activity appeared to be greater with 100 mM NaCl, subsequent  $\text{PS}_p$ -folding characterizations were carried out in buffer containing 100 mM NaCl. Uncatalyzed folding and  $\text{PS}_p$  binding measurements were performed under both conditions, and the results in the absence of 100 mM NaCl are given as Supporting Information (see Figure S1 and Table S1 in the Supporting Information).

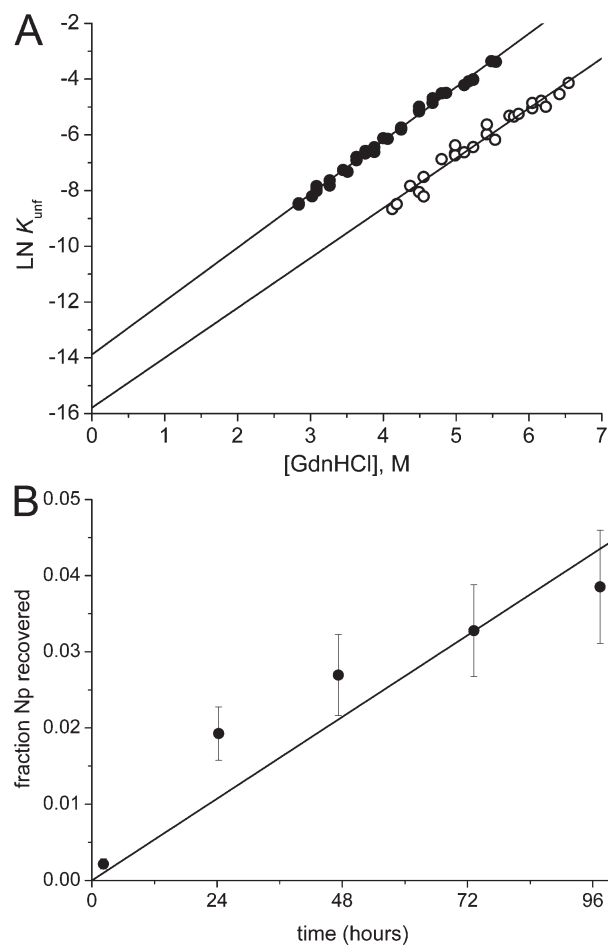


FIGURE 2: Kinetics of Np unfolding and uncatalyzed folding. (A) Np unfolding induced by GdnHCl, extrapolated to pure H<sub>2</sub>O, to estimate the rate of unfolding,  $k_{\text{unf}}$ , at 25 °C (closed circles) and 0 °C (open circles). (B) Uncatalyzed folding of Rp to Np, based on recovery of proteolytic activity, to estimate the rate of uncatalyzed folding,  $k_{f, \text{uncat}}$ . Error bars indicate the SD from four folding experiments.

**Native Pepsin Unfolding and Uncatalyzed Folding Rates.** To assess the kinetic stability of Np, the rate of unfolding,  $k_{\text{unf}}$ , was measured as a function of GdnHCl concentration and a plot of the natural logarithm of the data was extrapolated to obtain  $k_{\text{unf}}$  at 0 M GdnHCl (Figure 2A). Although it was previously reported that the denaturation of native pepsin is irreversible (6), the present study indicated that subnanomolar amounts of native protein could be detected using a fluorescence-based activity assay, thus allowing for the recovery of small fractions of the native state to be measured over a period of 4 days (Figure 2B). However, due to the slow rate of recovery, it was concluded that Np is irreversibly denatured on relevant time scales and thus equilibrium unfolding studies were not possible. Instead, comparing  $k_{\text{unf}}$  with the rate of uncatalyzed pepsin folding,  $k_{f, \text{uncat}}$ , provides a measure of the relative stability of Rp and Np. While Np was found to be kinetically stable, with a  $k_{\text{unf}}$  of  $1.4 \times 10^{-7} \pm 0.6 \times 10^{-7} \text{ s}^{-1}$  at 0 °C ( $t_{1/2 \text{unf}} = 58 \pm 29$  days), the rate of uncatalyzed folding was found to be comparably slow, with a  $k_{f, \text{uncat}}$  of  $1.3 \times 10^{-7} \pm 0.1 \times 10^{-7} \text{ s}^{-1}$  at 0 °C ( $t_{1/2 \text{fold}} = 64 \pm 6$  days). As folding/unfolding rates can be directly related to activation energies, this suggests that the free energies of Rp and Np are comparable at 0 °C. This finding is in agreement with previous DSC measurements, which showed that the  $T_m$  for Rp was  $\sim 5$  °C higher than that for Np (13), indicating that the native



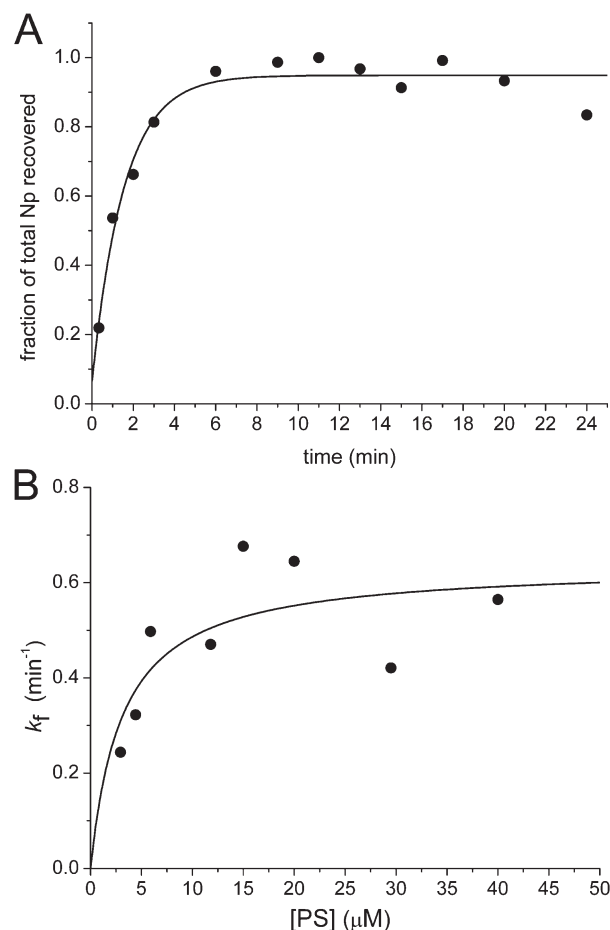


FIGURE 3:  $\text{PS}_p$ -catalyzed folding of Rp to Np. (A) Example of a kinetic trace of recovery of Np activity upon incubation with  $20 \mu\text{M}$   $\text{PS}_p$ , fit with a monoexponential function to obtain the folding rate,  $k_f$ . (B) Modified Michaelis–Menten model fit to  $k_f$  data obtained at various concentrations of  $\text{PS}_p$ .

form of pepsin is not the most thermodynamically stable form but is metastable. Np was found to be kinetically stable at  $25^\circ\text{C}$  as well, with a  $k_{\text{unf}}$  of  $9.0 \times 10^{-7} \pm 0.9 \times 10^{-7} \text{ s}^{-1}$  ( $t_{1/2 \text{ unf}} = 9 \pm 1$  days). Uncatalyzed folding measured in the absence of  $100 \text{ mM}$  NaCl (Supporting Information Figure S1 and Table S1) was characterized by a slower rate, corresponding to a lowering of the activation barrier in the presence of  $100 \text{ mM}$  NaCl by  $\sim 0.4 \text{ kcal/mol}$ , suggesting that shielding of electrostatic interactions may be important in stabilizing the folding transition state.

**Prosegment-Catalyzed Folding of Rp to Np.** In order to explain the ability of Np to fold *in vivo*, where folding would likely need to occur on a time scale of at least seconds to minutes and not days, it was hypothesized that the PS functions as a folding catalyst, enabling the formation of Np, which is then trapped as a kinetically stable fold upon removal of the PS. In order to test this hypothesis, an assay to measure the  $\text{PS}_p$ -catalyzed folding of pepsin was developed. Using  $\text{PS}_p$ , added exogenously to a solution of Rp, the rate of recovery of Np activity was measured as a function of  $\text{PS}_p$  concentration (Figure 3A and Supporting Information Figure S2). Although the folding reaction was carried out at pH 5.3, Np activity could only be detected when the sample was taken below pH 2, likely due to  $\text{PS}_p$  inhibition of recovered Np (see below). The rate of  $\text{PS}_p$ -catalyzed folding of Rp to Np versus  $\text{PS}_p$  concentration was fit according to a modified Michaelis–Menten formalism, resulting in a catalyzed folding rate,  $k_{\text{cat}}$ , of  $0.011 \pm 0.002 \text{ s}^{-1}$  and a

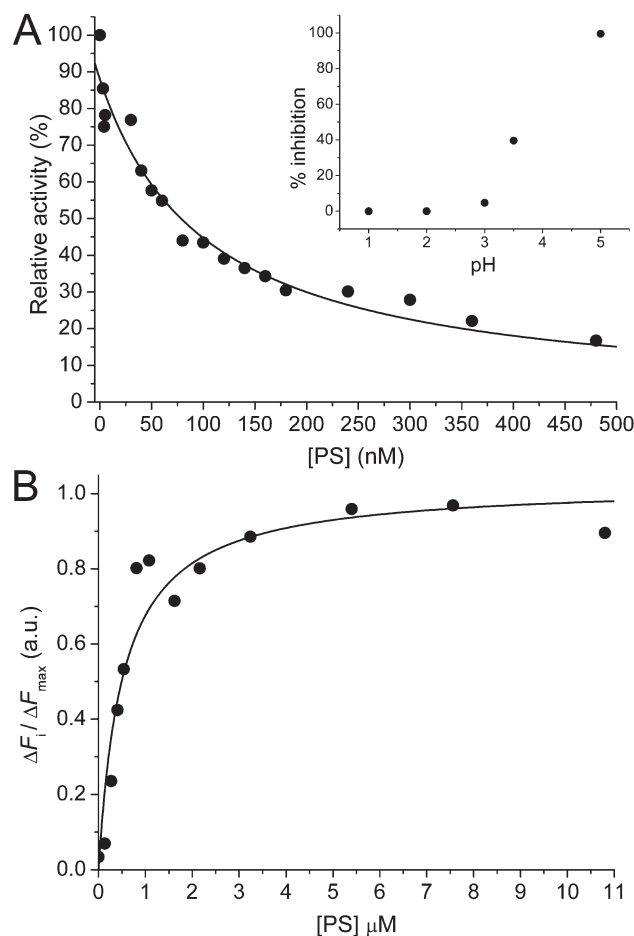


FIGURE 4:  $\text{PS}_p$  binding affinities for Np and Rp. (A)  $\text{PS}_p$  inhibition of Np at pH 5.3, fit with a competitive inhibitor model. The inset shows an example of the pH dependence of  $\text{PS}_p$  inhibition of Np, which was strong at pH 5 but was reduced to no detectable inhibition at pH  $\leq 2$ . (B)  $\text{PS}_p$  binding to Rp measured using the change in intrinsic tryptophan fluorescence of Rp upon interaction with  $\text{PS}_p$ .

Michaelis constant,  $K_M$ , of  $3.1 \pm 2.0 \mu\text{M}$  (Figure 3B). Similar to the use of the modified Michaelis–Menten model first described by Peters et al. (26), it was necessary to maintain the  $\text{PS}_p$  in excess over Rp to ensure that the  $\text{PS}_p$  was not depleted during the assay, which would otherwise occur as the  $\text{PS}_p$  has strong affinity for Np and thus functions as a single-turnover catalyst. An excess of  $\text{PS}_p$  was required in order to give pseudo-first-order folding kinetics. Compared with the uncatalyzed folding, which occurred on the order of days (Figure 2B), the  $\text{PS}_p$  proved to be an efficient catalyst in folding Rp to Np with a half-time of recovery of Np,  $t_{1/2 \text{ cat-fold}}$ , of  $65.2 \pm 9.5 \text{ s}$ , corresponding to an approximately 85000-fold increase in the folding rate. The catalytic efficiency, given as  $k_{\text{cat}}/K_M$ , which in this case describes the efficiency of the  $\text{PS}_p$  to act as a foldase of pepsin, was found to be  $3.4 \text{ s}^{-1} \text{ mM}^{-1}$ . Although this value is 3–6 orders less than typical  $k_{\text{cat}}/K_M$  values for enzyme reactions for optimized substrates (29), e.g., the  $k_{\text{cat}}/K_M$  of pepsin for the KPAAEFF( $\text{NO}_2$ )AL substrate used in this study is  $\sim 2000 \text{ s}^{-1} \text{ mM}^{-1}$  (22), this is likely a reflection of the relatively slow rate of protein folding compared to most enzyme-catalyzed reactions. Considering that a protein folding reaction involves the formation and breakdown of a vast number of interactions and conformational changes, a hydrolysis reaction appears simple in comparison. Thus, it can be concluded that the PS is well suited to catalyzing pepsin folding and likely has evolved to function particularly in this role.

**PS Affinity for Rp and Np.** In addition to acting as a folding catalyst, the PS<sub>p</sub> was found to be a strong inhibitor of Np activity at pH 5.3, binding with a  $K_i$  of  $33 \pm 3$  nM (Figure 4A). However, the inhibition was found to be strongly pH dependent (see inset in Figure 4A), with no inhibition detected at pH  $\leq 2$ . This pH dependence of PS inhibition allowed for the PS<sub>p</sub>-catalyzed conversion of Rp to Np to be followed at pH 5.3, based on the recovery of Np activity measured at pH 1.1, since no activity could be detected in the folded samples at pH 5.3. These results suggest that the PS<sub>p</sub>-Np interaction is likely controlled by electrostatic effects, as evidenced by the strong pH dependence of both PS<sub>p</sub> release upon reactivation and PS<sub>p</sub> inhibition of Np. Support for the importance of electrostatic interactions is given by the fact that the PS is rich in basic residues (13 basic and 2 acidic residues out of 44 total) whereas pepsin contains 43 acidic and only 4 basic residues. Thus, the PS is highly positively charged, and pepsin is highly negatively charged near pH 5, with pepsin losing its negative charge toward pH 2 (30).

As the error associated with the determination of the  $K_M$  value using the Michaelis–Menten fit (Figure 3B) was relatively large, a more precise measurement was obtained using fluorescence. To estimate the affinity of the PS<sub>p</sub> for Rp, the increase in intrinsic tryptophan fluorescence of Rp upon PS<sub>p</sub> binding was measured and used to calculate the dissociation constant,  $K_d$  (Figure 4B). The PS<sub>p</sub> displayed a moderate affinity for Rp, with a  $K_d$  of  $0.52 \pm 0.12$   $\mu$ M. Comparing the dissociation constant of the PS<sub>p</sub> for Rp versus that for Np (i.e.,  $K_d$  versus  $K_i$ ) shows that the PS has developed a greater affinity for the product than for the substrate of the pepsin folding reaction.

## DISCUSSION

**Pepsin Folding Landscape.** From the data presented in this study, the PS<sub>p</sub> is shown to catalyze folding from a stable denatured state to the native state before being removed in a pH-dependent dissociation step. The result is an otherwise kinetically stable native conformation that is incapable of refolding upon denaturation without the PS. To illustrate this situation more clearly, the energy landscape can be calculated from the equilibrium ( $K_{eq}$ ) and rate ( $k$ ) constants using the equations  $\Delta G = -RT \ln K_{eq}$  and  $k = (k_B T/h) \exp(-\Delta G^\ddagger/RT)$ . The activation free energy barriers to folding and unfolding were calculated using the rates of uncatalyzed folding and Np unfolding, respectively. The folding barrier in the presence of the PS<sub>p</sub> was determined using the catalyzed folding rate, and the PS<sub>p</sub> stabilization energies were obtained from the  $K_d$  and  $K_i$  values.

In the absence of the PS<sub>p</sub> (upper curve, Figure 5), Np is slightly destabilized relative to the denatured Rp state at 0 °C, in agreement with previous DSC data, which indicated that Np was destabilized by 0.9 kcal/mol relative to Rp at 25 °C (13). Inclusion of the PS<sub>p</sub> (lower curve, Figure 5) results in a large stabilization of both Rp and Np, but the additional 1.6 kcal/mol of Np-PS binding energy results in the Np-PS<sub>p</sub> state being stabilized by  $\sim 1.6$  kcal/mol over the Rp-PS<sub>p</sub> complex. Thus, in the presence of the PS<sub>p</sub> the native state becomes the more thermodynamically stable conformation. Compared with the Rp and Np binding energies, the PS<sub>p</sub> displayed the strongest affinity for the folding transition state, lowering the folding barrier by 14.7 kcal/mol, indicating that the primary role of the PS is to catalyze folding by stabilizing the folding transition state. The overall scenario that emerges is that PS<sub>p</sub>-catalyzed folding is thermodynamically driven to the Np-PS<sub>p</sub> state, after which

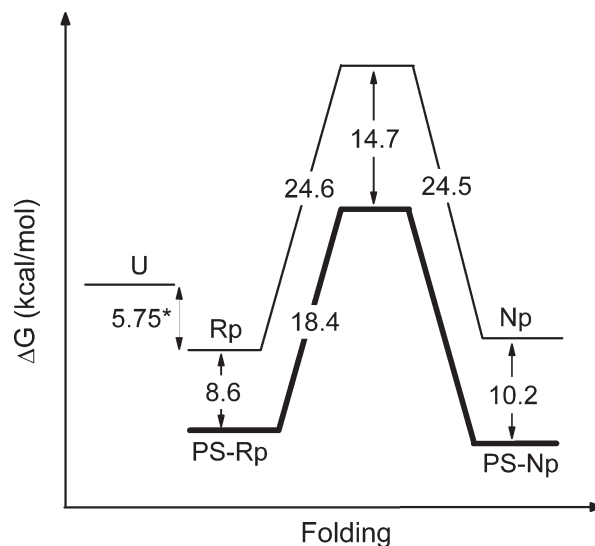


FIGURE 5: Free energy diagram summarizing the folding landscape of pepsin in the absence (thin line) and presence (thick line) of the prosegment peptide (PS<sub>p</sub>) at pH 5.3. The PS<sub>p</sub> lowers the energy barrier to native pepsin (Np) folding, increasing the folding rate by nearly  $10^5$ . In the absence of the PS<sub>p</sub>, Np is in a metastable state compared to denatured, refolded pepsin (Rp), while both Np and Rp are thermodynamically stable compared to the unfolded state (U). \*, previously measured using DSC (13). Folding and unfolding rates were measured at 0 °C, while binding constants were obtained at 25 °C. The lines are not drawn to scale.

removal of the PS<sub>p</sub> results in a 10.2 kcal/mol destabilization of Np and a 14.7 kcal/mol destabilization of the folding/unfolding transition state, resulting in a kinetically trapped native conformation. Although the free energy of Np is similar to that of Rp, Np is not an equilibrium state upon being folded and released from the PS and, therefore, is not thermodynamically stabilized; i.e., it would require weeks for Np to come to equilibrium with the stable Rp state due to the large folding and unfolding barriers ( $t_{1/2}$  of 64 and 58 days, respectively). Once equilibrium was finally reached, only 47% of the molecules would exist in the Np state (as derived from the equilibrium constant calculated using  $k_{unf}$  and  $k_{f,uncat}$  at 0 °C). As a consequence, the value of  $\Delta G_{Np-Rp}$ , whether it would be either a small positive or negative value, is insignificant compared to the folding/unfolding barriers which are on the order of 25 kcal/mol. In such a mechanism, the stability of the functional enzyme is ensured by the separation of the folding and the native state energy landscapes. That is, while the PS-catalyzed folding of pepsin is thermodynamically driven, once the PS is removed, the native state does not need to be the most thermodynamically stable state as long as there is a sufficient kinetic unfolding barrier to ensure the required functional lifetime.

**Evolution of Kinetic Stability.** To date, work on the serine peptidases  $\alpha$ -LP and SGPB has provided the most detailed evidence that some native protein states are actually kinetically stabilized as opposed to being thermodynamically stabilized (16). These enzymes have been characterized as being thermodynamically unstable ( $\alpha$ -LP) or marginally stable (SGPB) relative to their partially unfolded states, to have large free energy barriers to folding of 30 kcal/mol ( $\alpha$ -LP) and 23 kcal/mol (SGPB), and very slow rates of uncatalyzed folding, with  $t_{1/2} \approx 1300$  years ( $\alpha$ -LP) and  $t_{1/2} \approx 3$  days (SGPB) (17). Although pepsin,  $\alpha$ LP, and SGPB are structurally unrelated to each other, all three peptidases share the characteristics of kinetically trapped native states

that require the PS to accelerate folding to practical time scales, i.e., from uncatalyzed folding times of days, weeks, or years to PS-catalyzed folding times of seconds.

The degree to which the PS is required for folding to the native state places pepsin between  $\alpha$ LP and SGPB; for example, in terms of folding rate enhancement (catalyzed/noncatalyzed folding rate), the order of most to least is  $\alpha$ LP, pepsin, and SGPB, with rate enhancements of  $3 \times 10^9$  (17), 85000 and 400 (17), respectively. Thus it is likely that a spectrum of requirements for PS folding exists, from proteins completely dependent on the PS to proteins that can fold on their own but perhaps require the PS to enhance folding to time scales that allow for in vivo folding, i.e., by avoiding degradation, misfolding, and aggregation. PS-catalyzed folding may be quite relevant even in cases where it has been previously suggested that the PS is not required for folding. Several pepsin-like aspartic peptidases, including rennin (31), cathepsin D (32), and plasmepsin II (33), were found in the native form despite being expressed without the PS, while peptidase A (34) was not correctly folded when expressed in the absence of its PS. In such cases, it will be necessary to compare the folding kinetics in the presence and absence of the PS in order to quantitatively determine the role of the PS in folding and stabilization. For example, in the case of Tk-subtilisin, also a serine peptidase, it was found that although the protein could fold to the native form without its PS, in the presence of the PS the folding rate increased from 0.17 to 1.8 min<sup>-1</sup> (35).

Once folded, the PS is hydrolytically removed, resulting in an enzyme that is otherwise highly kinetically stable but is not stable in the reversible, thermodynamic sense. As such, these proteins are irreversibly unfolded but do not conform to the typical model for irreversible protein unfolding, i.e., the Lumry–Eyring model (1, 36):



where N and U are the native and unfolded states and F is an irreversibly modified state (i.e., due to proteolysis, chemical modification, or aggregation). Rather, the situation for pepsin and  $\alpha$ LP follows a different model:



where N and U are separated by a large energy barrier ( $\geq 25$  kcal/mol) and R is the thermodynamically stable denatured state to which the protein can fold upon crossing the barrier.

The separation of the folding and native conformation energy landscapes allowed by a PS-dependent folding mechanism likely has implications on the function of these enzymes. Indeed, it has been shown for  $\alpha$ LP and SGPB that a kinetic stabilization mechanism may allow for increased resistance to proteolytic degradation (17, 37). This latter scenario could certainly apply to pepsin, a digestive enzyme, where kinetic stability would be more relevant than thermodynamic stability to increasing the functional lifetime of the enzyme in the gastric fluid. Increasing kinetic stability via a large unfolding activation barrier is believed to be a general mechanism for prolonging the native lifetime in vivo (38).

**Structural Basis for Kinetic Stability in Pepsin.** Much remains to be discovered concerning the relationships between protein structure, dynamics, and kinetic stability, although there has been recent progress in this area, such as investigating the role of electrostatic interactions in modulating folding barriers (39, 40). Given the ability to manipulate Rp and Np, pepsin presents a novel model for studying the nature of the kinetic

barrier. While Np was found to be thermodynamically meta-stable compared to Rp, based on both unfolding and uncatalyzed folding rates (Figure 2) and from previous DSC data (13), Np is nonetheless lower in free energy than the completely unfolded state, by approximately 5 kcal/mol. Thus, the irreversibility of Np unfolding is due mainly to the large energy barrier separating this state from the unfolded and Rp states. The exact nature of what differentiates the structure of Np from Rp that accounts for this large energy barrier remains to be determined. DSC measurements indicated that upon thermal unfolding Rp had a reduced enthalpy ( $\Delta H_{cal}$ ) (13) and heat capacity change ( $\Delta C_p$ ) (Supporting Information Figure S3) compared to Np. As increased heat capacity has been related with an increase in solvation of nonpolar regions (41, 42), it is possible that there is a reorganization of hydrophobic residues to be more solvent exposed in Rp. The extent of structural reorganization that occurs in Rp in order to form Np remains unclear. Considering that the Rp state already contains considerable native-like structure (i.e., characterized by a similar radius of gyration using small angle neutron scattering and a large  $\beta$ -strand content determined by CD (13)), it is likely that the PS is required to stabilize a late-stage folding step. Current efforts are focused on comparing the structure and internal dynamics of Np and Rp as a model system to further elucidate the basis for protein kinetic stability.

In broader terms, PS-folding mechanisms may be considered within the “nucleation–condensation” model of protein folding (43), in which native structure propagates outward from a limited number of initial native-like contacts, or folding nucleation sites (44, 45). As the PS directly stabilizes the folding transition state (Figure 5), residues of the PS must form part of a nucleation site that then becomes integral to the folding transition state ensemble leading to the native state. It should be possible to define which PS residues form the folding nucleus using a  $\Phi$ -analysis approach (46), in which the effect of PS mutations on the transition state and native state stability are compared, relative to the wild type. Local structural changes that occur along the PS-catalyzed conversion of Rp to Np may be identified, as well as the possible structural origin(s) of the kinetic barrier.

## SUPPORTING INFORMATION AVAILABLE

Figures S1–S3 and Table S1 as described in the text. This material is available free of charge via the Internet at <http://pubs.acs.org>.

## REFERENCES

- Sanchez-Ruiz, J. M. (1992) Theoretical analysis of Lumry–Eyring models in differential scanning calorimetry. *Biophys. J.* 61, 921–935.
- Rodriguez-Larrea, D., Minning, S., Borchert, T. V., and Sanchez-Ruiz, J. M. (2006) Role of solvation barriers in protein kinetic stability. *J. Mol. Biol.* 360, 715–724.
- Sedláč, E., Žoldák, G., and Wittung-Stafshede, P. (2008) Role of copper in thermal stability of human ceruloplasmin. *Biophys. J.* 94, 1384–1391.
- Sohl, J. L., Jaswal, S. S., and Agard, D. A. (1998) Unfolded conformations of alpha-lytic protease are more stable than its native state. *Nature* 395, 817–819.
- Richter, C., Tanaka, T., and Yada, R. Y. (1998) Mechanism of activation of the gastric aspartic proteinases: pepsinogen, progastricsin and prochymosin. *Biochem. J.* 335, 481–490.
- Ahmad, F., and McPhie, P. (1978) The denaturation of covalently inhibited swine pepsin. *Int. J. Pept. Protein Res.* 12, 155–163.
- Privalov, P. L., Mateo, P. L., Khechinashvili, N. N., Stepanov, V. M., and Revina, L. P. (1981) Comparative thermodynamic study of pepsinogen and pepsin structure. *J. Mol. Biol.* 152, 445–464.



8. Lin, X. L., Loy, J. A., Sussman, F., and Tang, J. (1993) Conformational instability of the N- and C-terminal lobes of porcine pepsin in neutral and alkaline solutions. *Protein Sci.* 2, 1383–1390.
9. Tanaka, T., and Yada, R. Y. (2001) N-terminal portion acts as an initiator of the inactivation of pepsin at neutral pH. *Protein Eng.* 14, 669–674.
10. Konno, T., Kamatari, Y. O., Tanaka, N., Kamikubo, H., Dobson, C. M., and Nagayama, K. (2000) A partially unfolded structure of the alkaline-denatured state of pepsin and its implication for stability of the zymogen-derived protein. *Biochemistry* 39, 4182–4190.
11. Kamatari, Y. O., Dobson, C. M., and Konno, T. (2003) Structural dissection of alkaline-denatured pepsin. *Protein Sci.* 12, 717–724.
12. Jin, K. S., Rho, Y., Kim, J., Kim, H., Kim, I. J., and Ree, M. (2008) Synchrotron small-angle X-ray scattering studies of the structure of porcine pepsin under various pH conditions. *J. Phys. Chem. B* 112, 15821–15827.
13. Dee, D., Pencer, J., Nieh, M., Krueger, S., Katsaras, J., and Yada, R. Y. (2006) Comparison of solution structures and stabilities of native, partially unfolded and partially refolded pepsin. *Biochemistry* 45, 13982–13992.
14. Baker, D., Sohl, J. L., and Agard, D. A. (1992) A protein-folding reaction under kinetic control. *Nature* 356, 263–265.
15. Derman, A. I., and Agard, D. A. (2000) Two energetically disparate folding pathways of alpha-lytic protease share a single transition state. *Nat. Struct. Biol.* 7, 394–397.
16. Jaswal, S. S., Truhlar, S. M., Dill, K. A., and Agard, D. A. (2005) Comprehensive analysis of protein folding activation thermodynamics reveals a universal behavior violated by kinetically stable proteases. *J. Mol. Biol.* 347, 355–66.
17. Truhlar, S. M. E., Cunningham, E. L., and Agard, D. A. (2004) The folding landscape of *Streptomyces griseus* protease B reveals the energetic costs and benefits associated with evolving kinetic stability. *Protein Sci.* 13, 381–390.
18. Shinde, U. P., and Inouye, M. (1997) Protein memory through altered folding mediated by intramolecular chaperones. *Nature* 389, 520–522.
19. Bryan, P. N. (2002) Prodomains and protein folding catalysis. *Chem. Rev.* 102, 4805–4816.
20. Fisher, K. E., Ruan, B., Alexander, P. A., Wang, L., and Bryan, P. N. (2007) Mechanism of the kinetically-controlled folding reaction of subtilisin. *Biochemistry* 46, 640–651.
21. Gasteiger, E., Hoogland, C., Gattiker, A., Duvaud, S., Wilkins, M. R., Appel, R. D., and Bairoch, A. (2005) Protein Identification and Analysis Tools on the ExPASy Server, in *The Proteomics Protocols Handbook* (Walker, J. M., Ed.) pp 571–607, Humana Press, Totowa, NJ.
22. Tanaka, T., and Yada, R. Y. (1996) Expression of soluble cloned porcine pepsinogen A in *Escherichia coli*. *Biochem. J.* 315, 443–446.
23. Athauda, S. B. P., Matsumoto, K., Rajapakshe, S., Kuribayashi, M., Kojima, M., Kubomura-Yoshida, N., Iwamatsu, A., Shibata, C., Inoue, H., and Takahashi, K. (2004) Enzymic and structural characterization of nepenthesin, a unique member of a novel subfamily of aspartic proteinases. *Biochem. J.* 381, 295–306.
24. Kondo, H., Shibano, Y., Amachi, T., Cronin, N., Oda, K., and Dunn, B. M. (1998) Substrate specificities and kinetic properties of proteinase A from the yeast *Saccharomyces cerevisiae* and the development of a novel substrate. *J. Biochem.* 124, 141–147.
25. Dunn, B. M., Jimenez, M., Parten, B. F., Valler, M. J., Rolph, C. E., and Kay, J. (1986) A systematic series of synthetic chromophoric substrates for aspartic proteinases. *Biochem. J.* 237, 899–906.
26. Peters, R. J., Shiau, A. K., Sohl, J. L., Anderson, D. E., Tang, G., Silen, J. L., and Agard, D. A. (1998) Pro region C-terminus: protease active site interactions are critical in catalyzing the folding of alpha-lytic protease. *Biochemistry* 37, 12058–12067.
27. Jorgensen, R., Yates, S. P., Teal, D. J., Nilsson, J., Prentice, G. A., Merrill, A. R., and Andersen, G. R. (2004) Crystal structure of ADP-ribosylated ribosomal translocase from *Saccharomyces cerevisiae*. *J. Biol. Chem.* 279, 45919–45925.
28. Pace, C. N. (1986) Determination and analysis of urea and guanidine hydrochloride denaturation curves. *Methods Enzymol.* 131, 266–280.
29. Wolfenden, R. (2006) Degrees of difficulty of water-consuming reactions in the absence of enzymes. *Chem. Rev.* 106, 3379–3396.
30. Horn, D., and Heuck, C. (1983) Charge determination of proteins with polyelectrolyte titration. *J. Biol. Chem.* 258, 1665–1670.
31. Norman, J. A., Hadjilambri, O., Baska, R., Sharp, D. Y., and Kumar, R. (1992) Stable expression, secretion, and characterization of active human renin in mammalian cells. *Mol. Pharmacol.* 41, 53–59.
32. Fortenberry, S. C., and Chirgwin, J. M. (1995) The propeptide is nonessential for the expression of human cathepsin D. *J. Biol. Chem.* 270, 9778–9782.
33. Istvan, E. S., and Goldberg, D. E. (2005) Distal substrate interactions enhance plasmepsin activity. *J. Biol. Chem.* 280, 6890–6896.
34. van den Hazel, H. B., Kielland-Brandt, M. C., and Winther, J. R. (1993) The propeptide is required for in vivo formation of stable active yeast proteinase A and can function even when not covalently linked to the mature region. *J. Biol. Chem.* 268, 18002–18007.
35. Tanaka, S., Takeuchi, Y., Matsumura, H., Koga, Y., Takano, K., and Kanaya, S. (2008) Crystal structure of Tk-subtilisin folded without propeptide: requirement of propeptide for acceleration of folding. *FEBS Lett.* 582, 3875–3878.
36. Lumry, R., and Eyring, H. (1954) Conformational changes of proteins. *J. Phys. Chem.* 58, 110–120.
37. Jaswal, S. S., Sohl, J. L., Davis, J. H., and Agard, D. A. (2002) Energetic landscape of  $\alpha$ -lytic protease optimizes longevity through kinetic stability. *Nature* 415, 343–346.
38. Plaza del Pino, I. M., Ibarra-Molero, B., and Sanchez-Ruiz, J. M. (2000) Lower kinetic limit to protein thermal stability: a proposal regarding protein stability in vivo and its relation with misfolding diseases. *Proteins* 40, 58–70.
39. Halskau, O., Jr, Perez-Jimenez, R., Ibarra-Molero, B., Underhaug, J., Munoz, V., Martinez, A., and Sanchez-Ruiz, J. M. (2008) Large-scale modulation of thermodynamic protein folding barriers linked to electrostatics. *Proc. Natl. Acad. Sci. U.S.A.* 105, 8625–8630.
40. Pey, A. L., Rodriguez-Larrea, D., Bomke, S., Dammers, S., Godoy-Ruiz, R., Garcia-Mira, M. M., and Sanchez-Ruiz, J. M. (2008) Engineering proteins with tunable thermodynamic and kinetic stabilities. *Proteins* 71, 165–174.
41. Gómez, J., Hilser, V. J., Xie, D., and Freire, E. (1995) The heat capacity of proteins. *Proteins: Struct., Funct., Genet.* 22, 404–412.
42. Loladze, V. V., Ermolenko, D. N., and Makhadze, G. I. (2001) Heat capacity changes upon burial of polar and nonpolar groups in proteins. *Protein Sci.* 10, 1343–1352.
43. Daggett, V., Fersht, A., and R. (2003) Is there a unifying mechanism for protein folding? *Trends Biochem. Sci.* 28, 18–25.
44. Abkevich, V. I., Gutin, A. M., and Shakhnovich, E. I. (1994) Specific nucleus as the transition state for protein folding: evidence from the lattice model. *Biochemistry* 33, 10026–10036.
45. Broglia, R., Levy, Y., and Tiana, G. (2008) HIV-1 protease folding and the design of drugs which do not create resistance. *Curr. Opin. Struct. Biol.* 18, 60–66.
46. Fersht, A. R. (1995) Characterizing transition states in protein folding: an essential step in the puzzle. *Curr. Opin. Struct. Biol.* 5, 79–84.